Zeitschrift für Physikalische Chemie, **215**, 11, 1397–1411 (2001)

Investigations of Nuclear Quadrupole Interaction in $BaMgAl_{10}O_{17}:Eu^{2+}$

By M. Stephan[1,*], P. C. Schmidt[1], K. C. Mishra[2], M. Raukas[2], A. Ellens[3] and P. Boolchand[4]

[1] Darmstadt University of Technology, Darmstadt, Germany
[2] Central Research, OSRAM SYLVANIA INC., Beverly, MA, USA
[3] OSRAM, Research and Development, München, Germany
[4] University Of Cincinnati, Cincinnati, OH, USA

Dedicated to Prof. Dr. Dr. h.c. Wolf Weyrich on the occasion of his 60th birthday

(Received June 6, 2001; accepted June 18, 2001)

BAM / Barium Magnesium Aluminate / Nuclear Quadrupole Interaction / Phosphor / Electronic Band Structure / Luminescence / Europium

Local environments of divalent europium ions in β-lattice of barium magnesium aluminate, $BaMgAl_{10}O_{17}$ (BAM) have been investigated using a recently developed ab initio band structure method. This method is a variant of the full potential LMTO method. The reliability of this method for calculating electric field gradient (EFG) was tested in the case of aluminum oxide in corundum structure. The calculated EFGs at both cation and anion sites compare satisfactorily with those from other ab initio methods and from recent measurements. The nuclear quadrupole coupling constants for Eu^{2+} calculated by this method at various possible sites in BAM, when compared to recently measured ^{151}Eu Mössbauer spectroscopy results, suggest three locations for Eu^{2+}: a Beevers–Ross site, a mid-oxygen site and an anti-Beevers–Ross site. Energetically, the anti-Beevers–Ross site appears to be more stable than the other two sites.

1. Introduction

Nuclear quadrupole interactions from nuclear quadrupole resonance (NQR) spectroscopy, nuclear magnetic resonance (NMR) and Mössbauer spectroscopy have served as an important probe of the electronic structure of ionic crystals and semiconductors. These measurements usually yield two

* Corresponding author. E-mail: mstephan@pc.chemie.tu-darmstadt.de

parameters, a nuclear quadrupole coupling constant, (e^2qQ) and an asymmetry parameter η. The coupling constant (e^2qQ) describes the interaction between the nuclear quadrupole moment, eQ and electric field gradient (EFG) at the nuclear site, eq. Using first-principles methods, one can calculate the field gradient tensor at nuclear sites. Thus, the local environment of an impurity ion can be determined by comparing the calculated values of field gradient at various sites in the host with the measured values. Reliability of this approach depends critically on the accuracy to which the electronic wavefunction of the impurity ion and its surrounding can be calculated. In this paper, we have used data from ^{151}Eu Mössbauer measurements to determine the location and environment of divalent europium ions in $BaMgAl_{10}O_{17}:Eu^{2+}$, (BAM).

BAM is used as a blue phosphor in the fluorescent lamps. It emits in a broad band with the fluorescence peak near ~ 450 nm due to $5d$-to-$4f$ transition of Eu^{2+} ion. In contrast to the other two phosphors in the triblend, $Y_2O_3:Eu^{3+}$ (red) and $LaPO_4:Ce^{3+}$, Tb^{3+} (green), it is less stable with respect to oxidation at temperatures above ~ 400 °C and also to vacuum ultra-violet (VUV) radiation. During the last few years, there have been considerable efforts to understand how this phosphor degrades, and to improve its stability against VUV radiation and thermal degradation.

Understanding the mechanism of degradation requires a precise knowledge of the location and environment of europium ions in BAM. This is the primary motivation of this work. We recently investigated europium site occupancy (both location and oxidation states) in BAM using Mössbauer Spectroscopy at 4.2 K. This phosphor contains about 10.0% Eu ions in place of barium. The Mössbauer line shapes rule out a single substitutional site in BAM. The line broadening could both be quadrupolar or magnetic in origin. However, an analysis of the observed Mössbauer line shapes, assuming a quadrupolar interaction, reveals in most cases a pentamodal site distribution. There appears to be three divalent europium sites with quadrupole coupling constants, e^2qQ of 854.09, -1273.41, and -2499.52 MHz and isomer shifts (IS) of -17.61, -11.50 and -14.25 mm/s respectively, one weakly populated Eu^{3+} site with e^2qQ of -1437.50 MHz and an IS of -0.98 mm/s, and finally a fifth site with e^2qQ of -1020.07 MHz and IS of -8.69 mm/s. The fifth site is weakly populated, and its value lies outside the range of shifts for trivalent and divalent ions.

We will focus on the nuclear quadrupole interactions for ^{151}Eu ions at the three dominant divalent europium sites. Europium ions at these sites most likely contribute to luminescence from this lattice. The observed nuclear quadrupole coupling constants for Eu ions at these sites are larger than any other reported to date in any lattice. The pentamodal site distribution is indicative of the fact that Eu ions do not enter the lattice substitutionally. Most likely because of the radii mismatch between Ba and Eu ions, it is not at all surprising Eu ions cannot be stabilized at the regular site for large cations in β-alumina

structure. The observed nuclear quadrupole coupling constants will be used to model the sites and local environments of Eu in this lattice.

Three different theoretical approaches have been used in the past to calculate the EFG, *eq* at a nuclear site. In the first approach, the EFG at a nuclear site is calculated by summing over contributions from the surrounding ions to EFG at a particular site using a point charge model of the lattice. This lattice sum is corrected further by the Sternheimer anti-shielding factor to account for the contribution from the electronic distribution of the ion itself [1] arising from the response of the electronic distribution surrounding to the nucleus to the field created by the point charges. The second approach relies on an accurate calculation of EFG from the valence electron distribution, and contributions from the core electrons are estimated through the Sternheimer anti-shielding function [2]. The wavefunctions of the valence electrons are usually calculated by molecular orbital cluster or band structure methods. The third approach is based on calculating contributions to the EFG by all electrons and ions. The electronic part of EFG is calculated by using electronic distribution using a full potential supercell band structure method or molecular orbital cluster procedure. This is the most straightforward, ab initio approach; however, highly accurate wave functions are necessary to obtains results reliable enough to distinguish between different plausible sites [3].

There are two critical issues, which need careful consideration before applying a full potential band structure method to such complex systems as BAM with large unit cells and relatively open structure. First is the reliability of the approach itself in providing accurate wavefunctions. The wavefunctions and the associated electric field gradient tensor at the sites of interest should be fully converged with respect to all free parameters such as size of the basis sets etc. The suitability of the method can be easily tested by choosing simple systems, which can be studied without a huge computational effort, and by comparing the calculated EFG with the available data. In the present case, we have used α-alumina as a test case. The quadrupole coupling tensors (including the sign) at O and Al are known from ^{27}Al and ^{17}O nuclear quadrupole resonance spectroscopy [4–6]. There are also many theoretical investigations on the EFG tensor [7–14] reported in the literature that can be used to test results from this work.

The second aspect involves the applicability of such an approach to crystals with large unit cells and open structures. Recently, a new full potential band structure method has been developed which uses optimized minimal basis sets and which can handle crystals with large unit cells [15–17]. In the present paper, we used this method to calculate the nuclear quadrupole coupling constants for ^{151}Eu at three plausible sites in $BaMgAl_{10}O_{17}:Eu^{2+}$. These sites are known in the literature as the Beevers–Ross (BR) site where Ba atom is originally located, mid-oxygen (mO) site and anti-Beevers–Ross (a-BR) site. These sites will be described in detail in the following section. Results from our calculation suggest that divalent europium ions could occupy these sites in the host lattice.

2. Crystal structure

The crystalline structure of corundum is shown in Fig. 1, and the structural parameters are presented in Table 1. The crystal structure can be described as hexagonal closed packing of oxygen ions with aluminum ions occupying

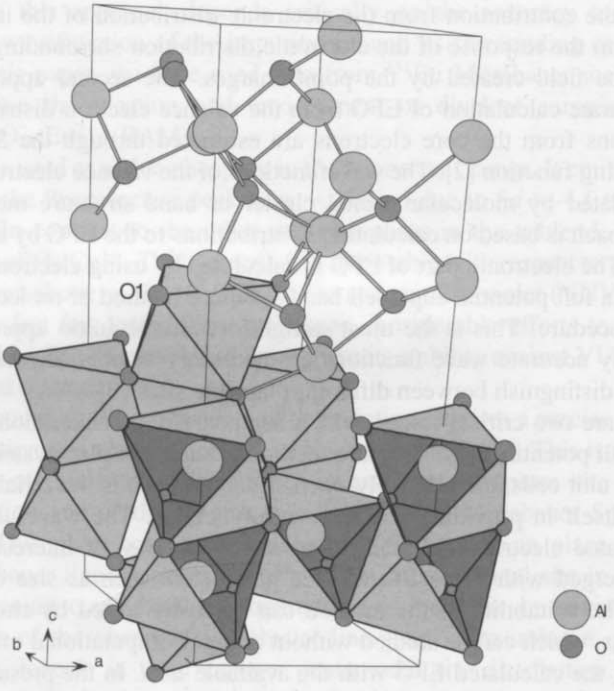

Fig. 1. Structure of α-Al_2O_3 (s. Table 1).

Table 1. Crystalographic data of α-Al_2O_3.

Formula sum	α-Al_2O_3
Crystal system	Hexagonal
Space group	$R\bar{3}c$ (no. 167)
Unit cell dimensions	$a = 4.7602(4)$ Å
	$c = 12.9933(2)$ Å
Z	6

Atom	**Wyck.**	**Occ.**	x	y	z
Al	12c	1	0	0	0.35216(1)
O	18e	1	0.30624(4)	0	1/4

two thirds of the octahedral interstices. Each AlO_6 octahedron is linked with three other octahedral through common edges and with one octahedron through a common face. The Al ions are displaced from the octahedral center towards the unshared faces. The Al–O distances are 1.972 Å and 1.855 Å and there are four non-equivalent O–O distances (2.525, 2.620, 2.726 and 2.867 Å) [18].

The crystalline structure of $BaMgAl_{10}O_{17}$ is shown in Fig. 2, and the structural parameters are presented in Table 2. The hexaluminates exhibit layer structures, which consist of the so-called conduction layers containing Ba ions and the spinel blocks stacking alternately along the *c* direction (see Fig. 2). The crystal structure of BAM is related to the β alumina structure of $NaAl_{11}O_{17}$. In the case of $BaMgAl_{10}O_{17}$, one Al^{3+} ion in the spinel block is replaced by a Mg^{2+} ion for charge-compensating the substitution of a Na^+

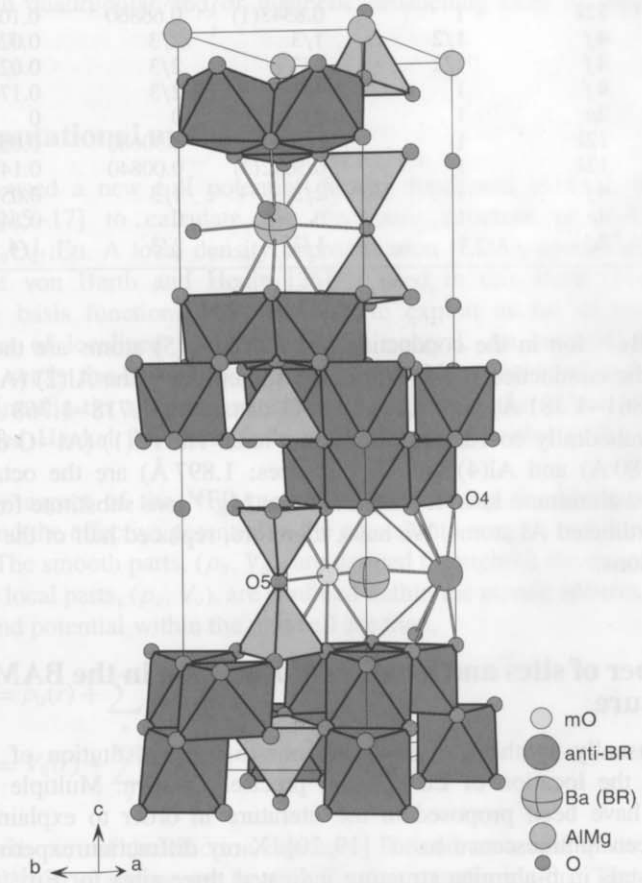

Fig. 2. Structure of $BaMgAl_{10}O_{17}:Eu^{2+}$ (s. Table 2).

Table 2. Crystalographic data of $BaMgAl_{10}O_{17}:Eu^{2+}$.

Formula sum	$BaMgAl_{10}O_{17}:Eu^{2+}$
Crystal system	Hexagonal
Space group	$P63/mmc$ (no. 194)
Unit cell dimensions	$a = 5.6275(7)$ Å
	$c = 22.658(7)$ Å
Z	2

Atom	Wyck.	Occ.	x	y	z
mO	6*h*	1/6	5/6	2/3	1/4
anti-BR_a	2*b*	1/2	0	0	1/4
anti-BR_b	6*h*	1/6	0.95900	0.91800	1/4
BR	2*d*	1/2	2/3	1/3	1/4
Ba1	2*d*	1/2	2/3	1/3	1/4
Al1	12*k*	1	0.8343(1)	0.66860	0.10544(4)
Al2	4*f*	1/2	1/3	2/3	0.02400(7)
Mg2	4*f*	1/2	1/3	2/3	0.02400(7)
Al3	4*f*	1	1/3	2/3	0.17416(7)
Al4	2*a*	1	0	0	0
O1	12*k*	1	0.1534(3)	0.30680	0.05152(9)
O2	12*k*	1	0.5042(3)	0.00840	0.14799(9)
O3	4*f*	1	2/3	1/3	0.05901(17)
O4	4*e*	1	0	0	0.14437(16)
O5	2*c*	1	1/3	2/3	1/4

ion by a Ba^{2+} ion in the conduction plane. The O(5) atoms are the oxygen atoms of the conduction layer. Within the spinel block, the Al(2) (Al–O distances: 1.861–1.881 Å) and Al(3) (Al–O distances: 1.718–1.768 Å) atoms are the tetrahedrally coordinated aluminum ions. The Al(1) (Al–O distances: 1.840–1.980 Å) and Al(4) (Al–O distances: 1.897 Å) are the octahedrally coordinated aluminum ions. It is believed that Mg^{2+} ions substitute for tetrahedrally coordinated Al atoms. We have, therefore, replaced half of the Al(2) by the Mg^{2+} ions.

3. Number of sites and location of Eu^{2+} ion in the BAM structure

BAM is usually synthesized assuming one-to-one substitution of Ba^{2+} by Eu^{2+}; yet, the location of Eu^{2+} is not precisely known. Multiple sites for europium have been proposed in the literature in order to explain the so-called "green luminescence band" [19, 20]. X-ray diffraction experiments on single crystals in β-alumina structure indicated three sites for Eu^{2+}, two being close to the anti-Beevers–Ross site (a-$BR_{a,b}$ in Table 2) and one at the

mid-oxygen site (mO) [21], see Fig. 2 and Table 2. Recent neutron diffraction measurements on BAM place the Eu^{2+} ions near the anti-Beevers–Ross site (a-BR_b in Table 2) [22]. Optical measurements lead to two different conclusions. Matsui *et al.* [23] concluded that there is only one luminescent center in BAM structure but three different sites were proposed for Eu^{2+} in $SrMgAl_{10}O_{17}$. Our studies on BAM doped with Sm^{2+} clearly showed the presence of more than one site [24]. However, the most convincing evidence for multiple sites comes from ^{151}Eu Mössbauer measurements. Cohen, Remeika and West proposed two sites, "A" and "B" for Na β-alumina doped with Eu^{2+} prepared by ion exchange method [25]. The "A" site is a typical Eu^{2+} site in oxygen environment but the "B" site with the smaller isomer shift (–14.6 mm/sec) is proposed to be a roomy site with more diffused 5*s* wave function [25]. Later Mössbauer measurements on BAM indicated similar possibility but no detailed analysis of Mössbauer spectra taking into account both quadrupolar and/or magnetic broadening exist to support these conjectures.

4. Computational method

We have used a new full potential density functional method, the 'NFP' method [15–17] to calculate the electronic structure of α-Al_2O_3 and $BaMgAl_{10}O_{17}:Eu$. A local density approximation (LDA), specifically a LDA variant of von Barth and Hedin [26] is used in this work. The method uses new basis functions [16] designed to exploit as far as possible the advantages of localized basis methods in general. An essential feature of the basis set is the use of atomic functions within non-overlapping atomic spheres (muffin-tin spheres) which are matched at the sphere boundaries to modified Hankel functions from which the singularities at the origin are removed.

A key aspect of the NFP method is partitioning the electronic charge density and the effective potential in the crystal into smooth and 'local' contributions. The smooth parts, (ρ_0, V_0), are defined throughout the entire unit cell, while the local parts, (ρ_ν, V_ν), are confined within the atomic spheres. The total density and potential within the unit cell are then,

$$\rho(r) = \rho_0(r) + \sum_\nu \rho_\nu(r) \tag{1}$$

$$V(r) = V_0(r) + \sum_\nu V_\nu(r)\,. \tag{2}$$

The smooth part of the electron density is defined on a real space mesh and is expanded in plane waves by fast Fourier transformation. The local part is expanded in spherical harmonics up to an angular-momentum cutoff l_{max}

and contains the components $\rho_{\nu,L}^{\text{true}}$ of the true electron density from the radial Schrödinger equation together with correction terms $\rho_{\nu,L}^{\text{corr}}$ which cancel out the contributions from the smooth part ρ_0 of the electron density inside the spheres,

$$\rho_\nu(r) = \sum_{L}^{L_{\max}} \left\{ \rho_{\nu,L}^{\text{true}}(r) - \rho_{\nu,L}^{\text{corr}}(r) \right\} . \tag{3}$$

The Coulomb and exchange-correlation potentials are treated similarly.

This separation procedure for the density and potential into smooth and localized parts is made in such a way that a relatively coarse real space mesh can be used for the smooth part of the density. A relatively low $l_{\max} = 2$ is then sufficient for the local part because the higher order contributions are included in ρ_0.

The orbital basis functions are combinations of atomic functions within the atomic spheres and are matched to modified Hankel functions $\tilde{h}_l(r)$ [16] at the sphere boundaries. The advantage of using the modified Hankel functions is that their behavior near the atomic sphere radius is closer to that of a regular atomic orbital than the usual Hankel function. The modified Hankel functions are optimized with respect to a smoothing parameter r_{sm} and the energy parameter ε. This choice of basis functions makes it possible for the method to achieve accurate results with a minimal basis set. Further details of this important feature of the basis set can be found elsewhere [16, 17]. A general description of the NFP method and code, including the manner in which the forces are computed can be found in [15].

The EFG tensor at the nuclear site $\boldsymbol{R}_\nu$ is described by the second derivative of the electrostatic potential V and can be calculated either from the electron density $\rho_\nu(\boldsymbol{r})$ or $V(\boldsymbol{r})$,

$$V_{i,k} := \left. \frac{\partial^2 V(\boldsymbol{r})}{\partial x_i \partial x_k} \right|_{\boldsymbol{r}=\boldsymbol{R}_\nu} = -\int \frac{\rho(\boldsymbol{r}) \left[3x_i x_k - r^2 \delta_{i,k} \right]}{r^5} \mathrm{d}\tau \tag{4}$$

where the x_i refer to position vectors in the crystallographic coordinate system. The resulting EFG has to be transformed to the principal axis system (x', y', z'). In the principal coordinate system, (x', y', z'), only the diagonal elements are needed to describe the tensor. The $V_{i',i'}$ are usually ordered according to $|V_{x',x'}| \leq |V_{y',y'}| \leq |V_{z',z'}|$. Due to Poisson's equation which require the tensor to be traceless, there are only two free parameter to describe the nuclear quadrupole interaction: $eq = eV_{z',z'}$ and the asymmetry parameter $\eta = (V_{x',x'} - V_{y',y'})/V_{z',z'}$.

In the NFP method, the dominant contribution to the EFG result from $\rho_{\nu,L}^{\text{true}}(r)$ inside the muffin-tin sphere. In all the cases studied here, contributions from other sources of charge distribution are found to be less than 5%.

5. Results and discussion

5.1 Aluminum oxide, α- Al_2O_3

The band structure calculations of corundum has been performed using the basis set Al($3s$, $3p$, $3d$) and O($2s$, $2p$). To calculate the EFG we have additionally used O($3d$) functions. The muffin-tin radii are chosen based on the minimum of the charge density between O and Al (basis set parameters are given in Table 3). In Fig. 3, we have shown the density of states (DOS) and the partial DOS of α-Al_2O_3 calculated by the NFP program. Fig. 4 shows the band structure of α-Al_2O_3. The upper valence band edge E_F is chosen to be the zero of the energy scale. The low energy peaks of the partial DOS at about -18.0 eV are the $2s$ like states of O. Above these bands are the valence states due to mostly $2p$-like states of O. The bonding character is predominantly ionic with weak admixture of Al $3s$- and $3p$-like states. The lower conduction states between

Table 3. Basis set parameters of α-Al_2O_3. r_{MT} is the Muffin–Tin radius, r_{SM} and E_{SM} are the choosen smoothing parameters of the non-singular Hankel functions (see [16]).

Species	r_{MT} [a_0]	Orbital	r_{SM}	E_{SM}
Al	1.94	s	2.238	−0.535
		p	2.076	−0.200
		d	1.339	−0.100
O	1.54	s	0.853	−1.279
		p	0.795	−0.353
		d	2.351	−0.100

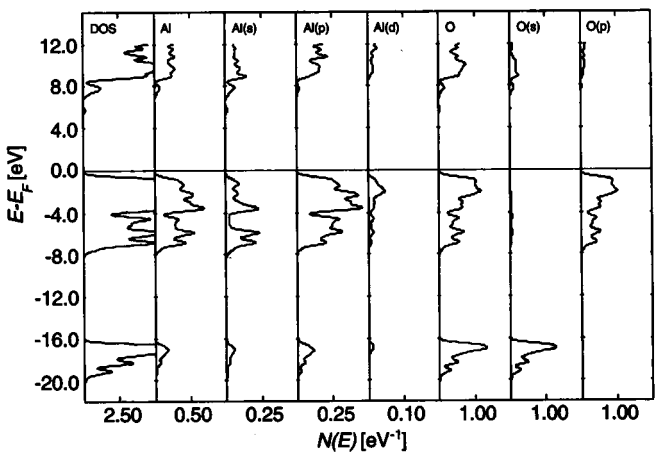

Fig. 3. Density of states (DOS) and partial density of states (PDOS) of α-Al_2O_3.

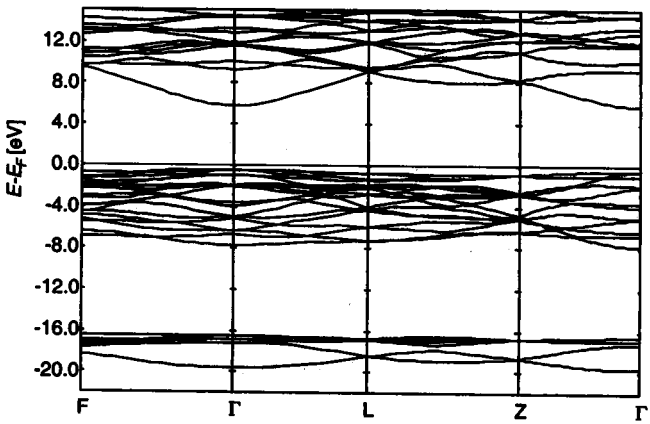

Fig. 4. Band structure of α-Al_2O_3.

8.0 and 12.0 eV are hybrid states of mostly $3s/3p$ character of Al and $2s/2p$ character of O. The ordering of the states is similar to Hartree–Fock [7, 13], tight-binding [14] and density functional [12] band structure calculations. Only the band widths are different for the different approaches. For example the band width of the O $2p$-like states is about 10 eV in Hartree–Fock [7] and 8 eV in the DFT approach. Furthermore it is a general problem in the density functional approach that the optical band gap ($E_g = 6.0$ eV for Al_2O_3) is lower than the experimental one ($E_g = 9.9$ eV for Al_2O_3) [18] and smaller than the Hartree–Fock result ($E_g = 16.0$ eV for Al_2O_3) [7].

In Table 4, we report the EFG tensor from the present calculation and compare with those from earlier calculations by cluster [10, 11] and band structure approaches [7, 12], and most importantly with the experimental results. In corundum, the Al site symmetry being 3 (C_3), the z' axis is oriented along the crystallographic c axis, and $\eta = 0$. Using the nuclear quadrupole

Table 4. Comparison of the calculated and measured electric field gradient tensor components $V_{t',t'}$ (in 10^{21} V m^{-2}) at the Al- and O-site, the asymmetry parameter η(O) and the angle $\varphi_{z',c}$(O) between z' and c in α-Al_2O_3.

Method	$V_{c',c'}$(Al)	$V_{z',z'}$(O)	η(O)	$\varphi_{z',c}$(O)
Hartree–Fock (Crystal) [7]	−0.476	+4.190	0.488	43.95
Cluster [10]		+6.566	0.546	47.58
Cluster [11]	−0.606	+2.603	0.532	48.18
DFT (LAPW) [12]	−0.617	+3.232	0.496	43.00
this work (NFP)	−0.690	+3.469	0.540	44.26
Experiment [16]	−0.655	+3.487	0.517	45.85

moment $Q(^{27}Al) = +15.1\,fm^2$ [27], one gets experimentally $V_{z',z'}(^{27}Al) = -6.553 \cdot 10^{23}\,V/m^2$ [18]. All DFT results including the present work agree within 95% with the experimental result.

The O site symmetry is 2 (C_2) and all the three component of the EFG tensor in the principal axis system are different. Using $Q(^{17}O) = -2.57\,fm^2$ [28] one gets $V_{z',z'}(^{17}O) = +34.872\,eV/m^2$ and $\eta = 0.517$ [18]. The x' axis is along the twofold axis (the crystallographic a axis) for O at (x(O), 0, 1/4) and the angle φ(O) between c and z' is equal to 45.85° [18]. On comparing the experimental EFG tensor with the theoretical results, we observe that the EFG at the anion site in contrast to that at the cation site is more sensitive to the chosen method than that at the cationic site. It is interesting that the NFP method using a minimal basis set leads to very satisfying results. Similar to the LAPW procedure, we obtain the right signs and orientation of the EFG tensors at the O and Al sites and furthermore there is a good agreement of the absolute values of the EFGs between the experimental and our theoretical results.

5.2 Barium magnesium aluminate (BAM), $BaMgAl_{10}O_{17}:Eu^{2+}$

We have calculated the band structure of $BaMgAl_{10}O_{17}$ and $BaMgAl_{10}O_{17}:Eu^{2+}$ using the atomic positions and cell parameter given in Table 2 and Fig. 2. The basis set parameters are listed in Table 5. The spin-polarization effects are not

Table 5. Basis set parameters of $BaMgAl_{10}O_{17}:Eu^{2+}$. r_{MT} is the Muffin–Tin radius, r_{SM} and E_{SM} are the choosen smoothing parameters of the non-singular Hankel functions (see [16]).

Species	r_{MT} [a_0]	Orbital	r_{SM}	E_{SM}
Eu	3.27	*s*	4.162	−0.458
		p	4.452	−0.200
		d	1.945	−0.200
Ba	3.60	*s*	5.016	−0.690
		p	1.424	−1.006
		d	2.130	−0.200
Al(1–4)	2.00	*s*	2.212	−0.528
		p	2.076	−0.200
		d	1.076	−0.200
O(1–5)	1.25	*s*	0.836	−1.249
		p	0.712	−0.296
Mg(2)	1.80	*s*	3.081	−0.451
		p	2.926	−0.200
		d	1.926	−0.200

included. Since the EFG depends on the total charge distribution, spin polarization is expected to contribute in the second order. We have used a spherically symmetric frozen $4f$-charge density of Eu (FOCA approximation in NFP, see [15]). In Fig. 5 we show the (DOS) for the calculated band structure (see also Fig. 6) of $BaMgAl_{10}O_{17}:Eu^{2+}$ with Eu at the BR site. In this model calculation, we replaced one of the two Ba atoms inside the unit cell by one Eu atom. Therefore, the Eu concentration in the modeled system is larger than that found in any phosphor.

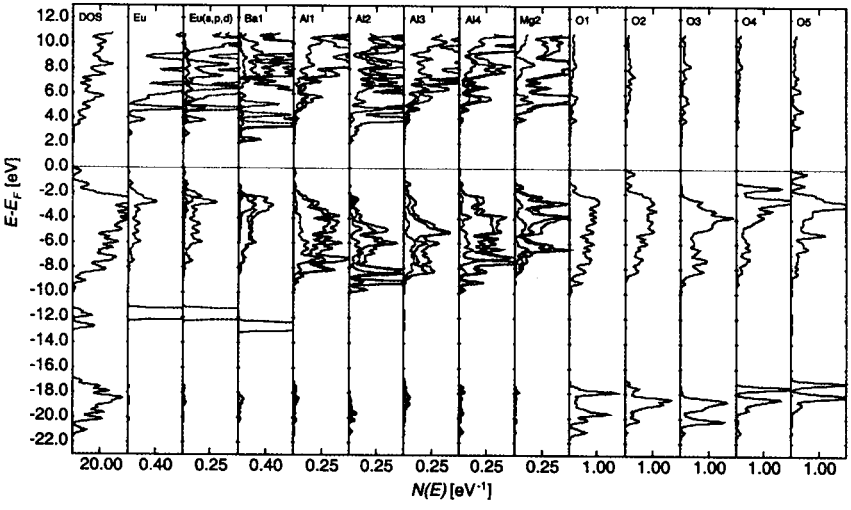

Fig. 5. Density of states (DOS) and partial density of states (PDOS) of $BaMgAl_{10}O_{17}:Eu^{2+}$.

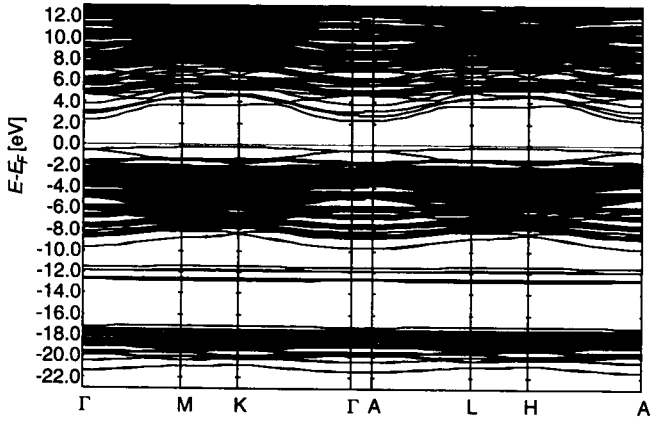

Fig. 6. Band structure of $BaMgAl_{10}O_{17}:Eu^{2+}$.

In Fig. 5, we note that the partial DOS of Al and of the spinel block O is similar to that of corundum. The partial DOS (PDOS) of O(2) and O(4) are slightly different from those of O(1) and O(3) because O(2) atoms are within the first coordination sphere of contacts Ba/Eu and the upper occupied states of O(4) are lone pairs forming slightly covalent bonds with Eu, if Eu is placed at the BR site. The lone pairs are even more pronounced for the oxygen of the conduction layer O(5). The PDOS of Mg on Al(2) positions are very similar to the PDOS of Al. There are two differences between the PDOS of Ba and Mg/Al. First, we find the $5p$ like states of Ba between the $2s$ and $2p$ like states of O and second, the predominant character of the low lying conduction bands of Ba are d like states instead of sp like states for Al and Mg. The PDOS of Eu are similar to the PDOS of Ba. One finds the Eu-$5p$ like states close to the $5p$ like states of Ba and the lowest conduction bands have predominantly $5d$ character. From the PDOS, we predict a optical band gap of about 4.0 eV which is smaller than the experimental band gap of about $\sim$ 6.5 eV [29]. (As mentioned above this is a general DFT problem.)

In order to calculate EFG at Eu site, one has to include contributions from the Eu electronic core, the $4f$ electrons and the valence electrons. Eu^{2+} ion being in $^8S_{7/2}$ state, we expect nearly zero contribution from the $4f$ electrons. Similarly, contributions from the core levels are also expected to be small compared to those from the distant ions and those from the hybridization of the valence electrons. We have also used the $6p$ rather than the $5p$ basis functions of Eu in order to describe polarization of the valence orbitals.

We have calculated the EFG tensor for the BR, the a-BR (a-BR_a and a-BR_b) and the mO sites. For Eu on the a-BR sites, there are large forces on O(4) if one uses the structural data of BAM to place Eu^{2+} in this lattice. Therefore, we have performed a local relaxation of O(4) in the lattice. The new site of O(4) is calculated to be (0, 0, 0.1295) which increases the Eu–O distance from the unrelaxed value 2.426 Å to a relaxed value of 2.759 Å. Typicaly the Eu^{2+}–O distance in oxides is between 2.540 Å and 2.938 Å.

In Table 6 the theoretical results for e^2qQ and η are listed along with the experimental results of e^2qQ_{exp}. It appears that the positive value of e^2qQ_{exp}

Table 6. Quadrupole coupling constants (e^2qQ in MHz) and free energy for the different locations of Eu^{2+} in $BaMgAl_{10}O_{17}:Eu^{2+}$.

Site	e^2qQ (Eu)	η(Eu)	E_{KS} [kJ/mol]	e^2qQ $(Eu)_{Exp}$
anti-BR_a, z(O4) = 0.1444	−4066.58	0.000	+875.289	
anti-BR_a, z(O4) = 0.1295	−1181.45	0.000	−802.106	−2499.52
anti-BR_b, z(O4) = 0.1444	−3388.36	0.024	+793.392	
anti-BR_b, z(O4) = 0.1295	−978.34	0.285	−779.198	
BR	−976.96	0.000	0.000	−1273.41
mO	+1149.20	0.213	+285.917	854.09

belongs to the mO site whereas the two negative values of e^2qQ_{exp} can be correlated to Eu at the BR and a-BR sites. For Eu at the a-BR site, the calculated EFG depends sensitively on the O(4)–Eu distance (Table 6). From our simulations we find a linear relation between the EFG and the O(4)–Eu distance, a change in the distance of 0.33 Å causes a change in the EFG of about 2600 MHz. We think that $e^2qQ_{exp} = -2499.52$ MHz belongs to the a-BR site but the defect structure is not perfectly simulated in our calculation.

To consider the relative thermodynamic stability of the different site occupancies of Eu we have also listed in Table 5 the total energy of the crystal where the energy locating Eu at the BR site is taken as the zero of our energy scale. One finds from this calculation that the most stable site is the a-BR site in accordance with the neutron diffraction results [22].

6. Conclusions

We have shown that a new variant of the full potential LMTO band structure program with a minimal basis set of non-singular Hankel functions can predict the electric field gradient tensor as well as other computationally intensive, ab initio methods. We have applied this method to study the electronic properties of Eu at various sites in barium hexaaluminate. A comparison of the calculated nuclear quadrupole coupling constants with those from ^{151}Eu Mössbauer measurements suggests that the divalent europium ions most likely occupy the BR, a-BR and mO sites in the β-alumina structure, the most stable site being the a-BR site. Our results also suggests that incorporation of Eu^{2+} into this lattice entails lattice relaxation possibly at all the sites. This should be investigated in greater detail in the future.

Acknowledgement

We thank Dr. Michael Methfessel from the Institut fuer Halbleiterphysik, Frankfurt/Oder, Germany for his very helpful support to incorporate the calculation of the electric field gradient tensor into his NFP program.

References

1. T. P. Das and P. C. Schmidt, Z. Naturforsch. **41a** (1986) 47.
2. K. D. Sen, P. C. Schmidt and A. Weiss, Z. Naturforsch. **41a** (1986) 37.
3. P. Blaha, K. Schwarz, P. Sorantin and S. B. Trickey, Comput. Phys. Commun. **59** (1990) 399.
4. R. V. Pound, Phys. Rev. **79** (1950) 685.
5. J. E. Rodgers, R. Roy and T. P. Das, Phys. Rev. A **14** (1976) 543.
6. A. H. Silver, T. Kushida and J. Lambe, Phys. Rev. **125** (1962) 1147.
7. L. Salasco, R. Dovesi, R. Orlando, M. Causa and V. R. Saunders, Mol. Phys. **72** (1991) 267.

8. A. Balzearotti, F. Antonangeli, R. Girlanda and G. Martino, Phys. Rev. B **29** (1984) 5903.
9. R. A. Evarestov, A. N. Ermoshkin and V. A. Lovchikov, Phys. Status Solidi B **99** (1980) 387.
10. A. S. Brown and M. A. Spackman, J. Phys. Chem. **96** (1992) 9200.
11. S. Nagel, J. Phys. C: Solid State Phys. **18** (1985) 3673.
12. B. Mayer, LAPW-calculation with the WIEN95 code, unpublished results.
13. M. Catti, G. Valerio, R. Dovesi and M. Causa, Phys. Rev. B **49** (1994) 14179.
14. T. J. Godin and J. P. LaFemina, Phys. Rev. B **49** (1994) 7691.
15. M. Methfessel, *NFP Manual*, Institut für Halbleiterphysik, Frankfurt (Oder) (1997).
16. E. Bott, M. Methfessel, W. Krabs and P. C. Schmidt, J. Math. Phys. **39** (1998) 1.
17. M. Methfessel, M. van Schilfgaarde and R. A. Casali, p. 114 in H. Dreysse Ed., *Electronic Structure and Physical Properties of Solids – The Use of the LMTO Method*, Lecture Notes in Physics, Vol. 535 (Springer-Verlag Berlin Heidelberg, 2000).
18. J. Lewis, D. Schwarzenbach and H. D. Flack, Acta Cryst. A **38** (1982) 733.
19. C. R. Ronda and B. M. J. Smets, J. Electrochem. Soc. **136** (1989) 570.
20. A. L. N. Stevels, J. Luminescence **17** (1978) 121.
21. W. Carrillo-Cabrera, J. O. Thomas and G. C. Farrington, Solid State Ion. **18** (1986) 19645.
22. S. R. Jansen, PhD-thesis, University of Eindhoven (1998).
23. H. Matsui, C. N. Xu, T. Watanabe, M. Akiyama and X. G. Zheng, J. Electrochem. Soc. **147** (2000) 4692.
24. A. Ellens, F. Zwaschka, F. Kummer, A. Meijerink, M. Raukas and K. C. Mishra, J. Luminescence **93** (2001) 147.
25. R. L. Cohen, J. P. Remeika and K. W. West, J. de Physique **c6-513** (1953) 35.
26. U. von Barth and C. Hedin, J. Phys. C **5** (1972) 1629.
27. H. D. Flack and C. van der Leun, Nucl. Phys. A **214** (1973) 1.
28. F. Ajzenberg-Selove, Nucl. Phys. A **281** (1977) 1.
29. The band gap is estimated from absorption measurements of undoped samples of BAM for both powder samples and single crystals.